Electronic Supplementary Material (ESI) for Physical Chemistry Chemical Physics.

Electronic Supporting Information

Large-scale Superhydrophobic Surface-enhanced Raman Scattering (SERS) Platform Fabricated via Capillary Force Lithography and Assembly of Ag Nanocubes for Ultratrace Molecular Sensing

Joel Ming Rui Tan,[^,†,#] Justina Jiexin Ruan,[†,#] Hiang Kwee Lee,[†,≠] In Yee Phang,[≠] Xing Yi Ling[†]*

† Division of Chemistry and Biological Chemistry, School of Physical and Mathematical Sciences, Nanyang Technological University, 21 Nanyang Link, Singapore 637371.

*≠ Institute of Materials Research and Engineering, A*STAR (Agency for Science, Technology and Research), 3 Research Link, Singapore 117602.*

^Interdisciplinary Graduate School, Nanyang Technological University, Singapore.

 # These authors contributed equally.

** To whom correspondence should be addressed. Email: xyling@ntu.edu.sg.*

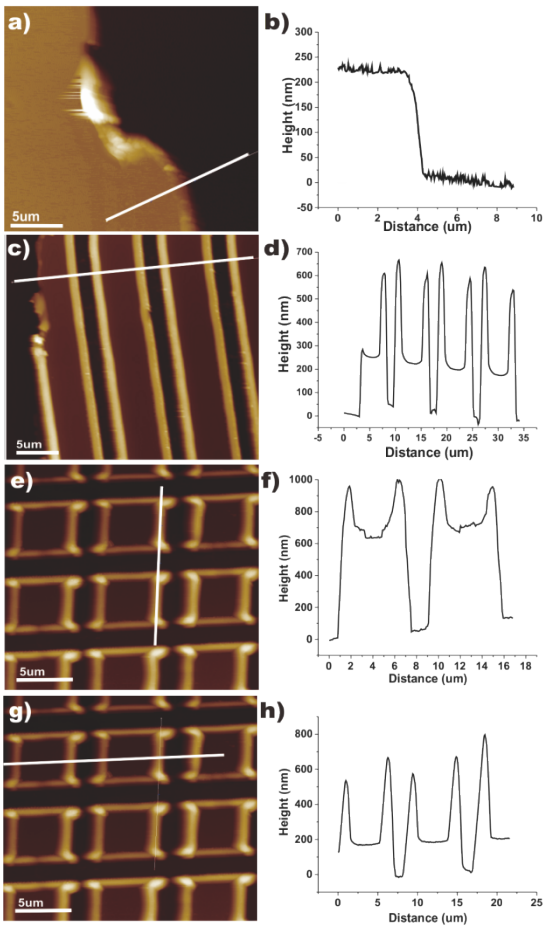

Figure S1. AFM images (left column) and height profile (right column) of 200 nm PMMA film at various fabrication steps. (a - b) 200 nm PMMA thin film and (c - d) linear patterns after first nanoimprinting. (e - f) and (g – h) are AFM profiles along the side walls and across box-like patterned template after the second nanoimprinting.

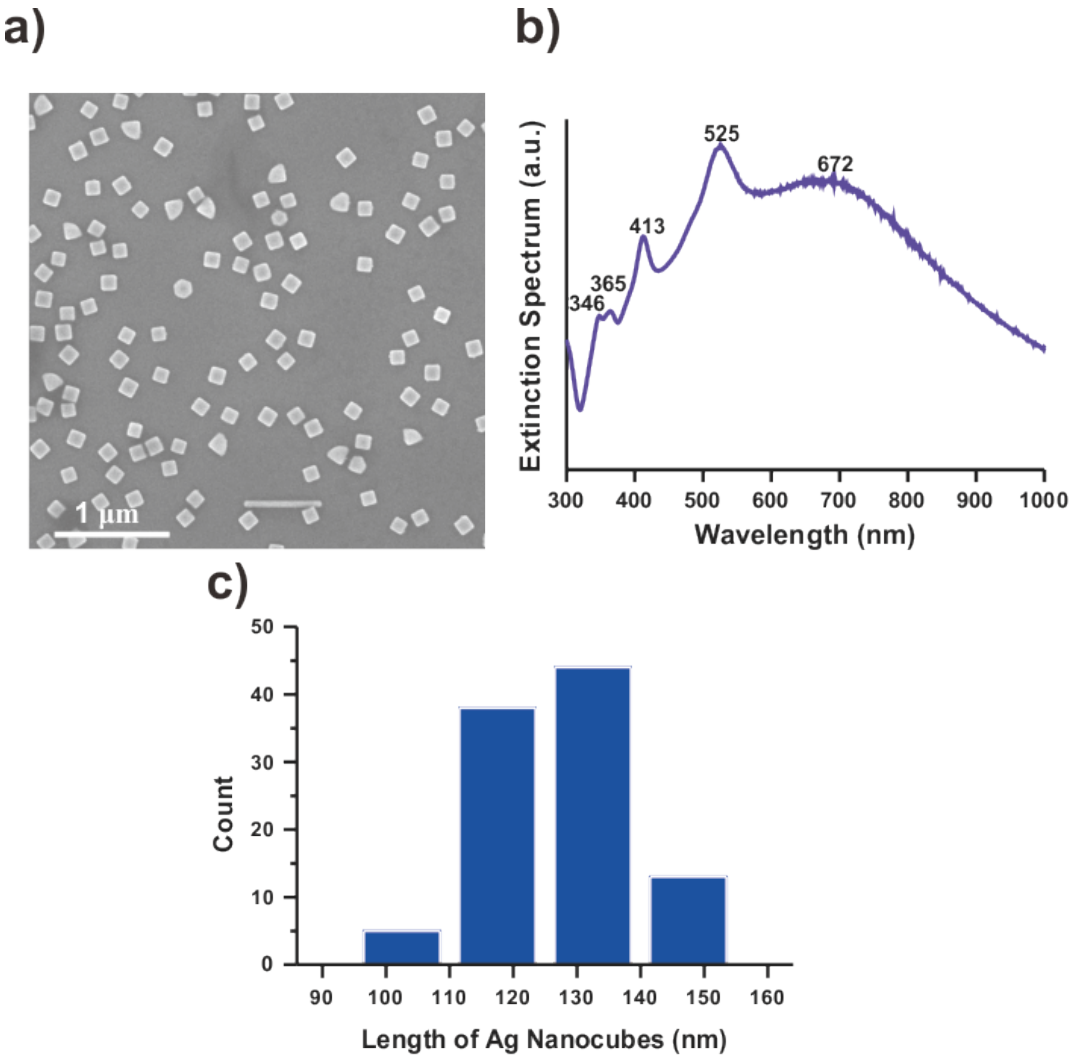

Figure S2. a) SEM image, b) UV-vis spectra and c) size distribution of Ag nanocubes used.

All the peaks in the extinction spectrum are characteristic localized surface plasmon resonances (LSPRs) of colloidal Ag nanocubes. Specifically, the peaks at approximately 346, 365, 413, 525 and 672 nm can be assigned to the octupole (346 nm and 365 nm), quadrupole (413 nm and 525 nm) and dipole resonances (672 nm) of Ag nanocubes, respectively.

Discussion on the selective aggregation of Ag nanocubes within the boxes

The selective aggregation of Ag nanocubes within the boxes is likely due to two factors. Firstly, the height of the box (~ 0.6 μm) is approximately 6-folds longer than the length of Ag nanocubes. Hence, capillary interaction of water with the interior hydrophilic alumina-coated walls will drive more Ag nanocubes into the boxes, forming multilayer aggregation instead of a monolayer. Secondly, the wall-to-wall length, approximately 5 μm, is much smaller than the capillary length of water such that surface tension of water will dominate over the effect of external forces,[1] like gravity and N_2 gas streaming, applied after the transfer of Ag nanocubes to remove residual water. Thus, Ag nanocube-containing water is likely to be trapped within the pore and subsequent drying will cause the formation of multilayer Ag nanocube.

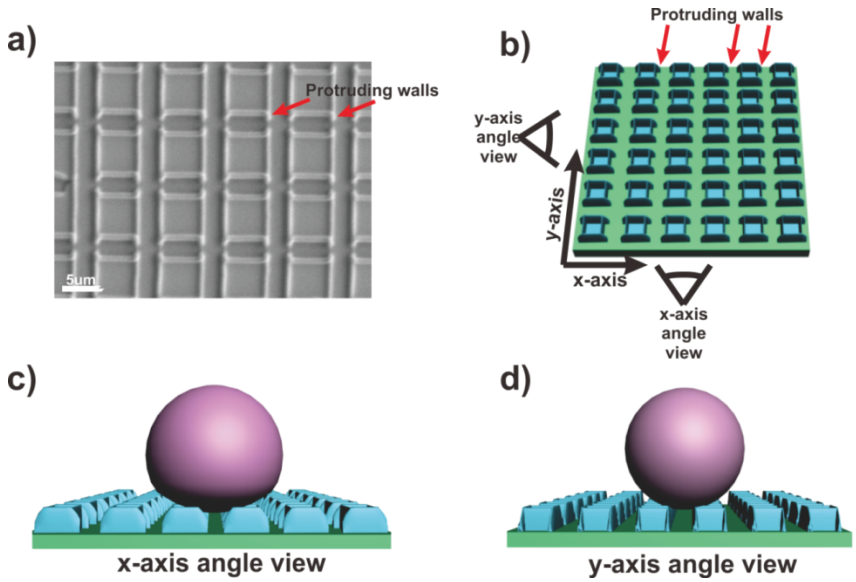

Figure S3. Illustration on the effect of the patterned template on static contact angles along different axes. (a) SEM image and (b) scheme of the patterned template. Effect of the patterned template on static contact angles viewed from the (c) x-axis angle and (d) y-axis.

The observation of two angles arises from the joining of the protruding corners of the patterns causing bidirectional (x-axis and y-axis) surface pattern. X-axis is define as the direction parallel to the protruding corners of the patterns while y-axis is define as the direction perpendicular to the protruding corners of the patterns. The droplet along the x-axis rests on lesser elevated walls as compared to y-axis (Figure S3). Due to the presence of perfluorodecanethiol on the wall surfaces, an area that possesses more elevated walls has a higher surface energy. Therefore the surface energy along the x-axis is lower as compared to y-axis. The resulting difference in surface energy along x and y axis leads to the observation of two contact angle with x-axis having a lower contact angle of 105±6° and y-axis having a contact angle of 138 ± 8°. Next, when a dense layer of Ag nanocubes are deposited on 200 nm PMMA patterns, a large increased in contact angles are observed, with contact angle along the x-axis increasing by ~ 50 % to 164 ± 5°, and contact angle along the y-axis increasing by ~ 22 % to 167 ± 7°. In contrast, superhydrophobicity cannot be achieved at early stages of the patterns fabrication with a flat PMMA surface having a contact angle of 111 ± 4 ° (Table S1). The increase in contact angle is due to the increase in surface roughness as shown earlier. In addition, after the deposition of Ag nanocubes, the disparity between both axial became negligible, thus indicating an increase in homogeneity of the surface roughness

a)

Raman shift (cm^{-1})	Raman mode
610	C-C-C in-plane bending
770	C-H out-plane bending
1182	C-H in-plane bending
1358	Aromatic C-C stretching
1504	Aromatic C-C stretching
1647	Aromatic C-C stretching

b)

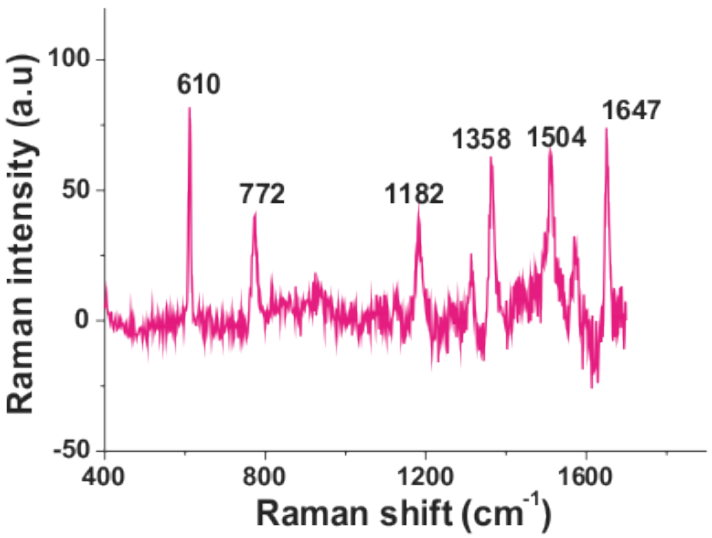

c)

$$\text{Analytical Enhancement Factor (AEF)} = \left[\frac{\text{SERS intensity}}{\text{Raman intensity}}\right] \times \left[\frac{\text{Analyte concentration for Raman measurement}}{\text{Analyte concentration for SERS measurement}}\right]$$

$$= \left[\frac{175}{82}\right] \times \left[\frac{10^{-4}}{10^{-17}}\right]$$

$$= 2 \times 10^{13}$$

Figure S4. (a) Table of peaks assignment for rhodamine 6G[2] and (b) Raman spectrum of rhodamine 6G. (c) Calculation of analytical enhancement factor on superhydrophobic SERS platform.

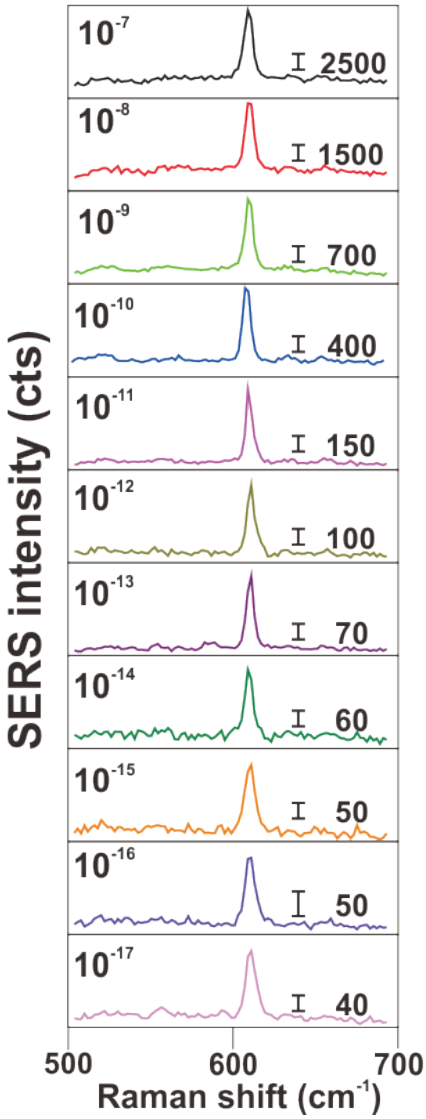

Figure S5. Application of superhydrophobic surface for ultratrace analysis using rhodamine 6G as probe molecule. SERS spectra of rhodamine 6G on superhydrophobic SERS substrate as a function of concentration ranging from 10^{-17} M to 10^{-7} M.

Reference

1. N. J. Shirtcliffe, G. McHale, S. Atherton and M. I. Newton, *Adv. Colloid Interface Sci.*, 2010, 161, 124-138.
2. P. Hildebrandt and M. Stockburger, *J. Phys. Chem.*, 1984, 88, 5935-5944.